RSC Advances

REVIEW

View Article Online
View Journal | View Issue

Cite this: *RSC Adv.*, 2021, **11**, 26354

Recent progress of effect of crystal structure on luminescence properties of Ce^{3+}–Eu^{2+} Co-doped phosphors

Mingjie Zheng, Zhijun Wang,* Xuejiao Wang, Jia Cui, Yao Yao, Mengya Zhang, Zhibin Yang, Lingwei Cao and Panlai Li*

Currently, the mechanism of Ce^{3+}–Eu^{2+} ET is frequently used to obtain color adjustable or white phosphors. Correspondingly, the ET efficiency from Ce^{3+} to Eu^{2+} becomes an important indication of the luminescent properties of phosphors. However, the ET efficiency calculated using the formula $\eta_{ET} = 1 - \frac{I_s}{I_{s0}}$ does not always match the emission spectra; the transmission efficiency of Ce^{3+} is high, but the emission efficiency of Eu^{2+} is low, depending on our investigation results. In addition to this problem, here we mainly review, on the basis of substantial examples, how to boost the actual ET efficiency of Ce^{3+}-to-Eu^{2+} and thus to improve the luminescent properties of phosphors through the rational design of layered crystal structure and the way of selective occupation of activator ions. Moreover, the possible physical mechanisms are proposed.

Received 17th June 2021
Accepted 20th July 2021

DOI: 10.1039/d1ra04700k

rsc.li/rsc-advances

1. Introduction

In recent years, a broad spectrum of new lighting materials has emerged, and white LED (WLED) materials have gradually replaced the traditional fluorescent lamps and incandescent lamps because of their energy-saving, environmental protection, high efficiency, long life and small size.[1] Due to these advantages, LEDs can be used in a wide range of areas, not only in solid state lighting, but also in other electronic devices such as displays. At present, researchers prefer to obtain color adjustable phosphors or white light phosphors by rational design of ET through rare earth (RE) ions co-doping such as Ce^{3+}–Eu^{2+}, Ce^{3+}–Mn^{2+}, Eu^{2+}–Mn^{2+}, Ce^{3+}–Eu^{2+}–Mn^{2+}, Ce^{3+}–Tb^{3+}–Mn^{2+} and Ce^{3+}–Tb^{3+}–Eu^{2+} systems, and so forth.[2–14] Among these systems, both Ce^{3+} and Eu^{2+} can emit 4f–5d transitions. Because their exposed 5d orbitals are susceptible to the crystal field environment, the luminescence range of Ce^{3+} can vary from the violet to red, and the spectral coverage of Eu^{2+} can even range from the ultraviolet to near-infrared, such as that in $K_3LuSi_2O_7$.[15] Therefore, rational design of Ce^{3+}-to-Eu^{2+} ET has become a popular way to obtain white light phosphors.

Over the past decades, many phosphors emitting adjustable color have been prepared by doping RE ions, and we could draw a conclusion that there are two main factors affecting the luminescent properties of phosphors: the kind of activator ions and the type of hosts. Both are indispensable for phosphors to achieve good luminescent properties. First, even for the same host, different kinds of activator ions will show different phenomena.[16–19] For example, solid state synthesis and tunable luminescence of Li_2SrSiO_4:Eu^{2+}/Ce^{3+} phosphors have been reported by Wei *et al.* Under excitation at 365 nm, the Ce^{3+} exhibits a broad blue emission ranging from 380 to 500 nm centered at 425 nm, while the Eu^{2+} exhibits a broad green emission in the range of 480–680 nm with center at 556 nm.[20] Synthesis, luminescence and ET of Ce^{3+}-to-Eu^{2+} of $SrSc_2O_4$:Ce^{3+}/Eu^{2+} phosphors have been reported by Zhao *et al.* Under excitation at 440 nm, $SrSc_2O_4$:Ce^{3+} shows a green emission peaking at ~535 nm, and the spectral coverage ranges from 475 to 675 nm. Under excitation at 523 nm, $SrSc_2O_4$:Eu^{2+} shows a red emission ranging from 650 to 775 nm with center at ~702 nm.[21] Photoluminescence, ET and tunable color of Ce^{3+}/Tb^{3+}/Eu^{2+} activated oxynitride phosphor with high brightness has been reported by Lv *et al.* $Ca_3Al_8Si_4O_{17}N_4$:Ce^{3+} shows a blue emission centering at 420 nm in the range of 340–525 nm, under excitation at 330 nm. And $Ca_3Al_8Si_4O_{17}N_4$:Eu^{2+} shows a blue emission in the range of 400–550 nm with center at 450 nm under excitation at 350 nm.[22] It can be seen that in the same host, different kinds of activator ions lead to different luminescence phenomenon.

In addition to the type of activator ions, the choice of host also has an impact on the luminescent properties of phosphors.[23–40] Eu^{2+} is a significant activator for luminescent materials because of its unique emission properties, so it has been researched in many hosts, as proved by the abundant examples such as $K_3LuSi_2O_7$:Eu^{2+}, $NaAlSiO_4$:Eu^{2+}, $Ca_2Al_3O_6F$:Eu^{2+}, $K_2BaCa(PO_4)_2$:Eu^{2+}, $Sr_9Mg_{1.5}(PO_4)_7$:Eu^{2+}, *etc.*15,41–44

College of Physics Science & Technology, Hebei Key Lab of Optic-Electronic Information and Materials, Hebei University, Baoding 071002, China. E-mail: wangzj1998@126.com; li_panlai@126.com; Tel: +86 312 5977068

First of all, with the variation of hosts, the emission wavelength of Eu^{2+} can change from the near-ultraviolet to near-infrared. Secondly, the thermal stability of phosphor materials is different in different hosts, which can be proved by the phosphors of $KBa_2(PO_3)_5$ (ref. 45) and $Ca_2Al_3O_6F$ (ref. 42) reported by Zhao and Xia, respectively. According to these two papers, the PL intensity of $Ca_2Al_3O_6F$:Eu^{2+} at 150 °C is only about 39% of its initial value (25 °C), but the PL intensity of $KBa_2(PO_3)_5$:Eu^{2+} at 150 °C retains 97% of its initial value.[42,45] In addition to the luminous color and the temperature stability of phosphors, host will also affect the quantum efficiency of phosphors. For example, in host $CaAlSiN_3$, the quantum efficiency of Eu^{2+} is as high as 95%, but in host $Ca_7Mg(SiO_4)_4$, the quantum efficiency of Eu^{2+} is only 30%.[23,29] Therefore, the effect of crystal field environment on the luminescence properties of Eu^{2+} is significant, including the position and half-peak width of luminescence, as well as the temperature stability and quantum efficiency of phosphors.

From the above discussion, we can conclude that host composition and crystal structure have a great effect on the luminescence properties of Eu^{2+}-singly doped phosphors, and in fact, for Ce^{3+}–Eu^{2+} co-doped phosphors, these factors also play a key role. The luminescence properties and ET mechanism of Ce^{3+}-to-Eu^{2+} have been analyzed by some research groups.[46–93] For instance, the ET processes of Ce^{3+}-to-Eu^{2+} in Ca_2PO_4Cl,[92] $Ba_3Ca_2(PO_4)_3F$[10] and $Ba_3Y(PO_4)_3$ (ref. 93) were once studied by our group. The overlaps between the emission spectra of Ce^{3+} and the excitation spectra of Eu^{2+}, the luminescence intensity and fluorescence lifetime of Ce^{3+} with changing the Eu^{2+} doping concentration were investigated in detail. After years of study in this field, we have a deeper understanding of the luminescence performance and ET mechanism of many Ce^{3+}–Eu^{2+} co-doped systems, and therefore putting forward the guiding ideology of improving the application of WLED. Despite the progress, there are still some problems to be further explored. Generally, the ET efficiency of Ce^{3+}-to-Eu^{2+} is calculated based on the luminescence intensity of Ce^{3+} together with the formula $\eta_{ET} = 1 - \frac{I_s}{I_{s0}}$. Sometimes, this calculated result is in accord with the emission spectra of Ce^{3+} and Eu^{2+}. For example, in the hosts $Ba_2MgSi_2O_7$,[63] $Ba_3Si_6O_{12}N_2$ (ref. 49) and $BaMg_2(PO_4)_2$,[87] their ET efficiency was calculated to be 90%, corresponding well to the emission spectra that the luminous intensity of Ce^{3+} decreased significantly and the luminous intensity of Eu^{2+} increased obviously. However, in the hosts such as $LiSr_4(BO_3)_3$,[72] $Ba_3Y(PO_4)_3$,[93] $Na_5Ca_2Al(PO_4)_4$,[56] although the ET efficiency of Ce^{3+}-to-Eu^{2+} was calculated to be 80% according to the formula $\eta_{ET} = 1 - \frac{I_s}{I_{s0}}$, it does not agree with the emission spectra of Eu^{2+} which did not increase correspondingly. Therefore, it is worth considering and exploring whether this phenomenon is related to the crystal structure and composition of host. If this problem can be solved, it may provide some clues and ideas when designing and selecting new Ce^{3+}–Eu^{2+} and even other RE ions co-doped materials.

2. Subject source

So far, there have some useful reviews summarizing on the Ce^{3+}–Eu^{2+} doped pc-WLED phosphors for solid-state lighting and displays such as those by Li,[94] Terraschke & Wickleder,[95] Xia,[96,97] Qiao,[98,99] Qin,[100] Wang,[101] Lin,[102] Li[103] *et al.* Especially, several recent reviews and articles have systematically

Table 1 Layer spacing, crystal structure, space group, and photoluminescence properties of Ce^{3+}–Eu^{2+} co-doped layered structured luminescent materials

Layered structure									
Compound	L (Å)	Crystal structure	Space group	λ_{em} (Ce^{3+})	λ_{em} (Eu^{2+})	X_c (Eu^{2+})	R_c (Å)	Mechanism of ET	Ref.
$BaMg_2(PO_4)_2$	9.691	Trigonal	$P\bar{1}$	412 nm	447 nm	0.05	30.7	d–d	87
$Ba_{1.2}Ca_{0.8}SiO_4$	7.352	Trigonal	$P\bar{3}m2$	385 nm	450 nm	0.02	17.11		80
$SrSi_2O_2N_2$	7.231	Trigonal	$P\bar{1}$	395 nm	530 nm	0.02	26.05	d–d	17
$Ba_3Si_6O_{12}N_2$	6.784	Trigonal	$P3$	393 nm	526 nm	0.01	25.11	d–d	49
Li_2SrSiO_4	5.522	Trigonal	$P3$	420 nm	570 nm	0.01	27.62		20
$Ba_3Si_6O_9N_4$	6.784	Trigonal	$P3$	420 nm	520 nm	0.005	24.86	d–d	59
$Ba_2MgSi_2O_7$	5.406	Tetragonal	$P\bar{4}21m$		560 nm	0.04			63
$Sr_2Al_2SiO_7$	5.264	Tetragonal	$P\bar{4}21m$	415 nm	510 nm	0.03	18.3	d–d	57
$Ca_2Mg_{0.25}Al_{1.5}Si_{1.25}O_7$	5.05	Tetragonal	$P\bar{4}21m$	409 nm	520 nm	0.025		d–d	46
$Ca_2Mg_{0.5}AlSi_{1.5}O_7$	5.036	Tetragonal	$P\bar{4}21m$	410 nm	525 nm	0.015	26.71	d–d	4
$Ca_8Mg_3Al_2Si_7O_{28}$	5.029	Tetragonal	$P\bar{4}21m$		535 nm	0.01			40
$BaSi_2O_2N_2$	7.592	Orthorhombic	$Pbcn$	390 nm	495 nm	0.05	24.87	d–d	79
Ba_2SiO_4	7.513	Orthorhombic	$Pmcn$		505 nm	0.03			39
Sr_2SiO_4	6.148	Orthorhombic	$Pmnb$	406 nm	469 nm	0.01			24
$CaAlSiN_3$	5.636	Orthorhombic	$Cmc2_1$	580 nm	650 nm	0.008	22.75	d–d	85
Ba_2ZnS_3	4.21	Orthorhombic	$Pnam$	498 nm	660 nm	0.008	32.7	d–d	77
$Ba_4Si_6O_{16}$	6.983	Monoclinic	$P12_11$	442 nm	497 nm	≥0.025			66
$LiBaBO_3$	6.416	Monoclinic	$P12_1/c_1$	430 nm	530 nm	0.02	25.06		70
$Ca_2Si_5N_8$	6.991	Monoclinic	$C1c1$	465 nm	595 nm	0.0035	22.27	d–d	50

introduced the design, the optical properties and the application of pc-WLED phosphors with the emphasis on the dependence of luminescence properties on the crystal structure and composition of host.[104–135] Different from these work, here we provide a new perspective to review the recent reports. In order to find out the reason why the ET efficiency calculated according to the formula $\eta_{ET} = 1 - \frac{I_s}{I_{s0}}$ does not match the Eu^{2+}'s emission spectra, we have carefully investigated the crystal structure, luminescence location, quenching concentration and other related information of many hosts, as exhibited in Tables 1 and 2. As the hosts with similar crystal structure and composition have similar luminescent phenomenon, so we focus on the crystal structure of these hosts. Moreover, it was found that the actual ET efficiency of Ce^{3+}-to-Eu^{2+} in the hosts with layered crystal structure is higher than those with non-layered crystal structure. Based on these results, the crystal structures of all hosts involved in this paper are then divided into two categories: layered structure and non-layered structure, in the following discussion.

As shown in Fig. 1, for the hosts with layered crystal structure, high, medium and low actual ET efficiency of Ce^{3+}-to-Eu^{2+} separately make up 65%, 20% and 15% of the whole cases. In contrast, high, medium and low actual ET efficiency of Ce^{3+}-to-Eu^{2+} make up 31%, 24% and 45% of all the hosts with non-layered crystal structure, respectively. It is obvious that the actual ET efficiency of Ce^{3+}-to-Eu^{2+} in the hosts with layered crystal structure is significantly higher than that with non-layered crystal structure.

According to previous reports, in the host with layered crystal structure, the quenching concentration is relatively large, which indicates that this structure can inhibit the quenching effect of activated ions to a certain extent. For the hosts with layered crystal structure, the cation layer is separated by other anion groups or other cationic polyhedrons, thus widening the distance between the same cationic sites. According to the diagram of concentration quenching process (Fig. 2), we found that when the doping concentration of activator ions is relatively low, the average distance of activators is relatively large. Under such conditions, it is hardly any interaction between activators, so less ions forms one luminescence center that is shown in the left part of Fig. 2. With the increase of activator ions concentration, the distance between activator ions is shortened, which thus increases the probability of ET, causing the energy loss of activator ions through ET step by step, thus multiple ions will form one equivalent luminescence center that is shown in the right part of Fig. 2.[6] Due to the particularity of crystal structure, the distance between the same cations in the

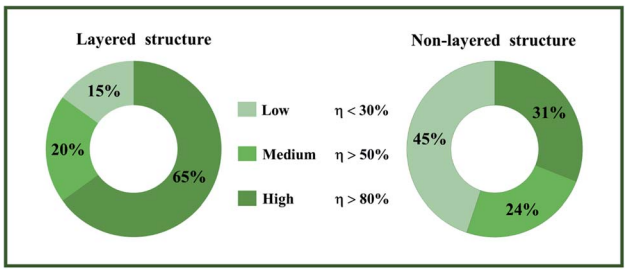

Fig. 1 The proportion of the host with high, medium and low ET efficiency in the hosts with layered and non-layered crystal structure.

Table 2 Crystal structure, space group, and photoluminescence properties of Ce^{3+}–Eu^{2+} co-doped non-layered structured luminescent materials

Non-layered structure

Compound	Crystal structure	Space group	λ_{em} (Ce^{3+})	λ_{em} (Eu^{2+})	X_c (Eu^{2+})	R_c (Å)	Mechanism of ET	Lattice site of Eu^{2+}	Ref.
Ca_2PO_4Cl	Orthorhombic	*Pbcm*	370 nm	460 nm	0.07	14.7	d–d	Ca1	92
$SrSc_2O_4$	Orthorhombic	*Pnam*	535 nm	702 nm	0.04	14.498	d–d	Sr	21
$BaSiO_3$	Orthorhombic	$P2_12_12_1$	404 nm	570 nm	0.02			Ba	48
$SrB_2Si_2O_8$	Orthorhombic	*Pnma*	373 nm	440 nm	0.01	25.82	d–d	Sr	51
$Ca_{1.65}Sr_{0.35}SiO_4$	Orthorhombic	$P2_1cn$	465 nm	538 nm		17	d–d	Sr1 to Sr6	88
$Ca_3MgSi_2O_8$	Monoclinic	$P2_1/a$	400 nm	470 nm	0.03	18.64	d–d	Ca	60
$Ca_3Si_2O_7$	Monoclinic	$P12_1/a_1$	490 nm	625 nm	0.0125	13.7	d–d	Ca1 to Ca3	75
$Ca_4(PO_4)_2O$	Monoclinic	$P112_1$	460 nm	356 nm	0.01	23.8	d–d	Ca1 to Ca8	83
Sr_2LiSiO_4F	Monoclinic	$P2_1/m11$	400 nm	465/520 nm	0.0075			Sr1 and Sr2	74
Ca_2BO_3Cl	Monoclinic	$P2_1/c$	410 nm	573 nm	0.015		d–d	Ca1 and Ca2	55
$Ca_3SiO_4Cl_2$	Monoclinic	$P2_1/c$	400 nm	505 nm	0.006			Ca	67
$Sr_5(PO_4)_3Cl$	Hexagonal	$P6_3/m$	370 nm	443 nm	0.1	21	d–d	Sr2	65
$La_5Si_2BO_{13}$	Hexagonal	$P6_3/m$	380 nm	519 nm	0.05	10.66		La1 and La2	54
$Ba_3Ca_2(PO_3)_3F$	Hexagonal	$P6_3/m$	387 nm	508 nm	0.05	17.506	d–d	M1 and M2	10
$Ca_4Y_6O(SiO_4)_6$	Hexagonal	$P6_3/m$	426 nm	527 nm	0.1	18.7	d–d	—	69
$Ca_9Al(PO_4)_7$	Trigonal	*R3c*	356 nm	445 nm	0.01	12.64	d–d	Ca	78
$Sr_3B_2O_6$	Trigonal	$R\bar{3}ch$	434 nm	574 nm	0.002	30.7	d–d	Sr1 and Sr2	53
$Ca_9Y(PO_4)_7$	Trigonal	*R3c*	342 nm	493 nm	0.005	30.644	d–d	Ca1 to Ca3, Y	52
$LiSr_4(BO_3)_3$	Cubic	$Ia\bar{3}d$	423 nm	612 nm	0.004	29.14	d–d	Sr1 and Sr2	72
$Sr_3Gd(PO_4)_3$	Cubic	$I4\bar{3}d$	374 nm	518 nm	0.01	32.02	d–d	Sr/Gd	62
$Ba_3Y(PO_4)_3$	Cubic	$I4\bar{3}d$	398 nm	520 nm	0.01	19.5	d–d	Ba/La	93

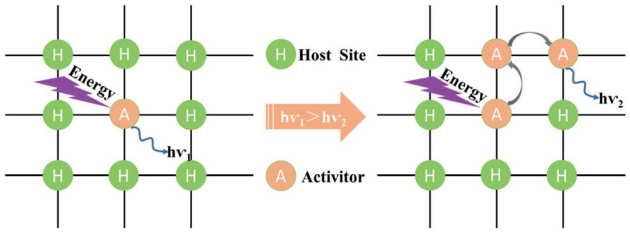

Fig. 2 Diagram of concentration quenching process.

hosts with layered crystal structure is far, therefore reducing the probability of ET of activator ions and make the emission efficiency of Eu^{2+} is higher.

In order to find out the further explanation, the hosts with layered crystal structure listed above are investigated in detail. Owing to the special layered crystal structure, the same cations are far apart from each other, which effectively inhibits the concentration quenching effect of activator ions. So for the layered structure, the larger the spacing between layers (L) is, the more obvious the effect of inhibiting the concentration quenching of activator ions is. And then, the higher the doping concentration of activator ions is, the greater the luminous intensity is. Since the activator ion Eu^{2+} is sensitive to the changes of surrounding crystal field environment, the quenching concentration (QC) of activator ion is expected to change when changing the spacing between layers (L). The hosts with layered crystal structure can be divided into three categories according to crystal system: tetragonal, trigonal and orthorhombic (Fig. 3a–c). All the hosts listed in Fig. 3a are tetragonal with space group $P\bar{4}21m$, those listed in Fig. 3b are trigonal with space group $P\bar{3}$ or $P\bar{1}$, and the hosts listed in Fig. 3c are all orthorhombic. The insets in Fig. 3a and b are the crystal structure diagrams of hosts seen from different directions. In Fig. 3c, although the hosts are all layered structures, they can be divided into the layered structures with and without connecting bonds due to different space groups. It can be seen from Fig. 3 that the QC of Eu^{2+} increases with the increase of spacing between layers (L) in the same crystal system. It is further proved that with the increase of distance between the cationic sites occupied by activator ions, the effect of inhibiting the concentration quenching of activator ion becomes greater. Therefore,

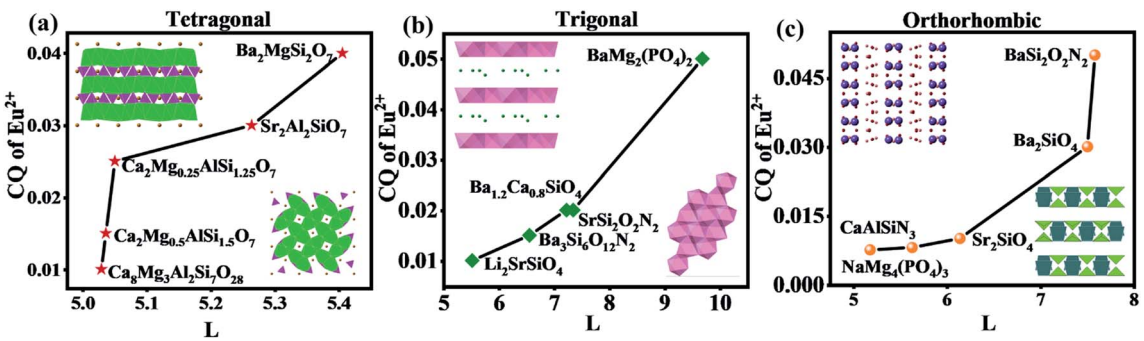

Fig. 3 The relationship between the spacing between layers (L) and the QC of Eu^{2+} in (a) tetragonal, (b) trigonal and (c) orthorhombic host.

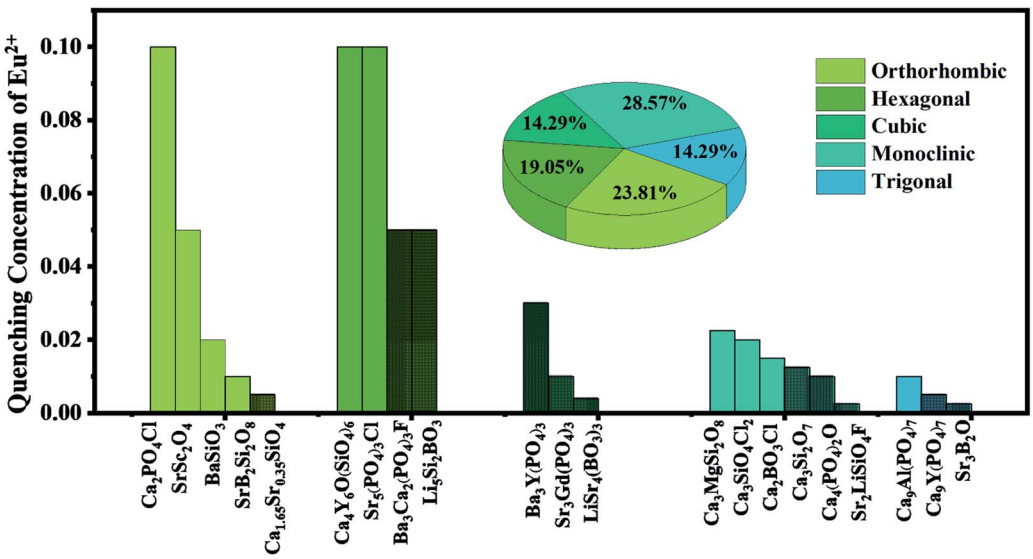

Fig. 4 Effect of selective occupancy of activator ions on the QC of Eu^{2+} in non-layered hosts.

the doping concentration of activator ions becomes higher and the luminescence property of phosphors becomes better.

It should be noticed, however, that the luminescence properties of some hosts with non-layered structure are also excellent, which can be explained as follows. Some of the hosts with non-layered structure are separated by the surrounding anionic groups, while others have gaps between the same cations by means of the selective occupancy of activator ions, which is called the interstitial structure. This structure can also indirectly increase the distance between the same cationic sites, followed by the inhabitation of the quenching effect of activator ions and the increase of doping concentration of activator ions. As shown in Fig. 4, the 21 hosts listed can be divided into five categories according to their crystal systems: orthorhombic, hexagonal, cubic, monoclinic and trigonal. And the proportions of these five crystal systems are 23.81%, 19.05%, 14.29%, 28.57% and 14.29%, respectively. In Fig. 4, different colors represent different crystal systems. For the hosts within the same crystal system, the unshadowed portion represents the host with interstitial structure, while the shadowed portion represents the host whose crystal lattice is occupied by activator ions that is tightly connected (we call it the cluster structure). It can be seen from the diagram that the QC of activator ions in the interstitial structure is higher than that in the cluster structure for all crystal systems. This further demonstrates that the larger the distance between the cationic sites occupied by the activator ions is, the greater the effect of inhibiting the concentration quenching of activator ions is. And then, the greater the doping concentration of activator ions is, the better the luminescence property of phosphors is.

As is well known, the emitting intensity of activator ions will be weak if the doping concentration is quite small. Therefore, inhibiting the concentration quenching of activator ions can increase the doping concentration of activator ions, thus enhancing the intensity of luminescence. Based on this conclusion, we found that the design of layered crystal structure and the selective occupation of activator ions can inhibit the concentration quenching of activator ions and improve the luminescent properties of Ce^{3+}–Eu^{2+} co-doped phosphors to some extent. Next, we will take some reported hosts as an example for specific analysis.

3. Effects of crystal structure on luminescence properties of Ce^{3+}–Eu^{2+} co-doped phosphors

3.1 Improving luminescence performance of Ce^{3+}–Eu^{2+} co-doped phosphors by designing selective occupancy of activator ions

A large amount of Ce^{3+}, Eu^{2+} singly-doped and Ce^{3+}–Eu^{2+} co-doped phosphors have been reported. According to these reports, Ce^{3+} and Eu^{2+} are sensitive to the changes of surrounding crystal field environment. Specifically, their luminescence location, spectral range, quenching concentration and thermal stability will be different with the variations of crystal field environment. Therefore, it is a common way to adjust the luminescent properties of phosphors by changing the crystal field environment around activator ions. In particular, the method of improving the luminescent properties of phosphors by designing the occupation sites of activator ions has been intensively studied.[127–135]

Since the luminescent properties of Ce^{3+} or Eu^{2+}-singly doped phosphors can be improved by the method of activator ion selective occupation, the luminescence properties of Ce^{3+}–Eu^{2+} co-doped phosphors is also expected to be improved using the same way. Currently, a large number of Ce^{3+}–Eu^{2+} co-activated halogenated phosphate hosts have been found. $Ba_3Ca_2(PO_4)_3F$[10] and $Sr_5(PO_4)_3Cl$[65] are two representatives, and both of them belong to the apatite structure system. As shown in Fig. 5a and d, the crystal structure of them belongs to the hexagonal system with $P6_3/m$ space group. There are two kinds of cationic sites in $Ba_3Ca_2(PO_4)_3F$, which are signed as M1(Ca1/Ba1) and M2(Ca2/Ba2) to facilitate the following discussion. The M1 sites are surrounded by nine oxygen anions with local symmetry C_3, forming a tricapped trigonal prism. The M2 sites are seven-fold coordinate surrounded by six oxygen anions and one fluorine anion with C_s point group symmetry. While in $Sr_5(PO_4)_3Cl$, the cationic sites are signed as Sr1 and Sr2. From Fig. 5a and d we can see that each Sr1/M1 sites is surrounded by anionic polyhedron and Sr2/M2, every three Sr2/M2 polyhedrons form a cluster with F^- ion through the vertex angle, and each cluster is separated by Sr1/M1 polyhedron and anionic polyhedron.

It can be seen from the structure diagram that if the doped RE ions occupy both lattice sites, the distance between activator ions is likely to be smaller, which increases the possibility of concentration quenching as discussed above. As shown in Fig. 5b and e, the emission spectrum of $Ba_3Ca_2(PO_4)_3F$:Eu^{2+} contains asymmetrically broad green-emission band from 400 to 650 nm, which is ascribed to the two different sites of Eu^{2+}.[10] According to the previous analysis of crystal structure, this spectrum can be decomposed well into two Gaussian bands with peaks centering at 498 and 534 nm, respectively. The Eu2(M2) site will lead to a shorter wavelength band due to the presence of F^- anion, so the 498 nm emission comes from the Eu2(M2) site and the 534 nm emission comes from the Eu1(M1) site.[10] In contrast, in the host $Sr_5(PO_4)_3Cl$, the emission spectrum of Eu^{2+} shows a symmetrically narrow emission band from 400 to 500 nm, which indicates that Eu^{2+} is likely to enter only one of the cation sites and therefore indirectly pull the distance between the same lattices, making the same cationic lattices farther apart and reducing the probability of ET between activator ions.[65]

According to the above inference, the doping concentration of Eu^{2+} in $Sr_5(PO_4)_3Cl$ is higher than that in $Ba_3Ca_2(PO_4)_3F$. It can be seen from Fig. 5c and f that in $Sr_5(PO_4)_3Cl$, with the increase of Eu^{2+} doping concentration, the luminescence intensity of Ce^{3+} decreases greatly, while the luminescence intensity of Eu^{2+} increases sharply. When the doping concentration of Eu^{2+} reaches $x = 0.5$, the emission intensity of Eu^{2+} still does not show a downward trend.[65] In contrast, the emission intensity of Ce^{3+} in $Ba_3Ca_2(PO_4)_3F$ decreases with the increase of Eu^{2+} doping concentration, and the emission

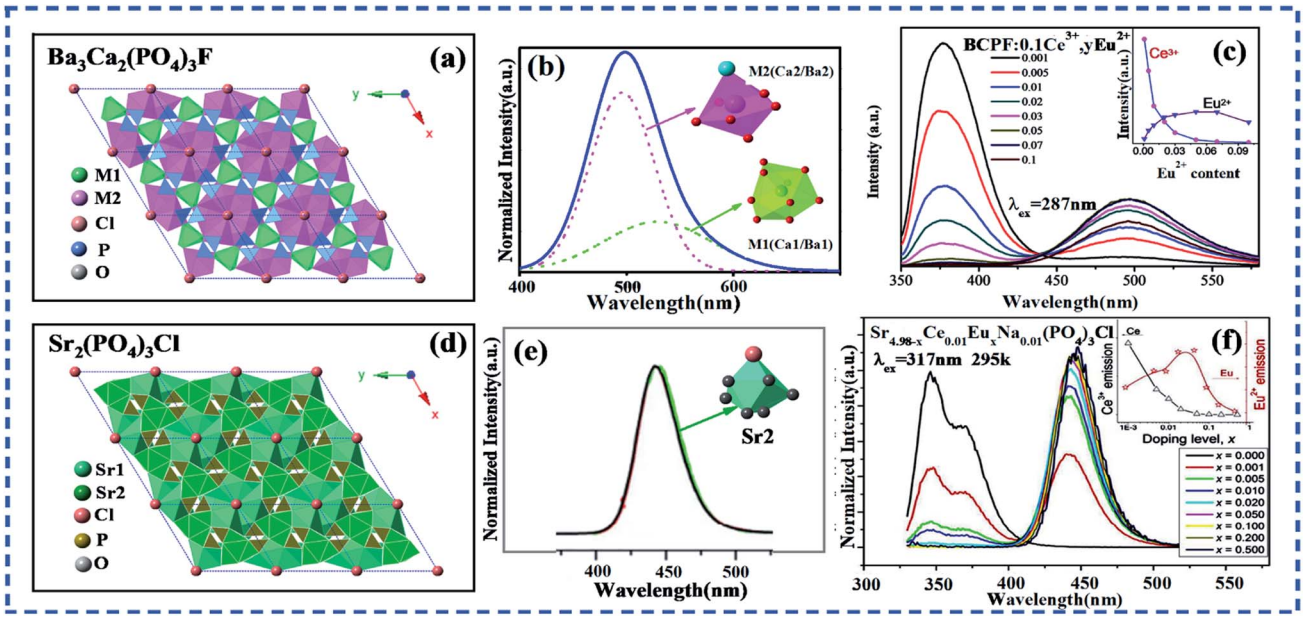

Fig. 5 (a) The crystal structure of $Ba_3Ca_2(PO_4)_3F$. (b) The PL spectra of $Ba_3Ca_2(PO_4)_3F:Eu^{2+}$ phosphors (c) the PL spectra of a series of $Ba_3Ca_2(PO_4)_3F:0.1Ce^{3+},xEu^{2+}$ phosphors with different Eu^{2+} concentrations excited at 287 nm. The inset shows the emission intensity of Ce^{3+} and Eu^{2+} with the increase of Eu^{2+} concentration in $Ba_3Ca_2(PO_4)_3F$ phosphors. (d) The crystal structure of $Sr_5(PO_4)_3Cl$. (e) The PL spectra of $Sr_5(PO_4)_3Cl:Eu^{2+}$ phosphors. (f) The PL spectra of a series of $Sr_5(PO_4)_3Cl:0.01Ce^{3+},xEu^{2+}$ phosphors with different Eu^{2+} concentrations excited at 317 nm. The inset shows the emission intensity of Ce^{3+} and Eu^{2+} with the increase of Eu^{2+} concentration in $Sr_5(PO_4)_3Cl$ phosphors. (Reproduced with permission from ref. 10 and 65, copyright 2013, 2017, *J. Mater. Chem. C, J. Alloys Compd.*)

intensity of Eu^{2+} increases first and then decreases with the maximum at $x = 0.05$.[10] Therefore, no matter in terms of the QC of Eu^{2+} or the actual ET efficiency of Ce^{3+}-to-Eu^{2+}, $Sr_5(PO_4)_3Cl$ is superior to $Ba_3Ca_2(PO4)_3F$. This result proves that the previous inference is correct. The distance between cation lattices does affect the quenching concentration of Eu^{2+} and the ET efficiency of Ce^{3+}-to-Eu^{2+}. When the cation lattices are far apart, the ET efficiency of Ce^{3+}-to-Eu^{2+} is relatively high. It is because the

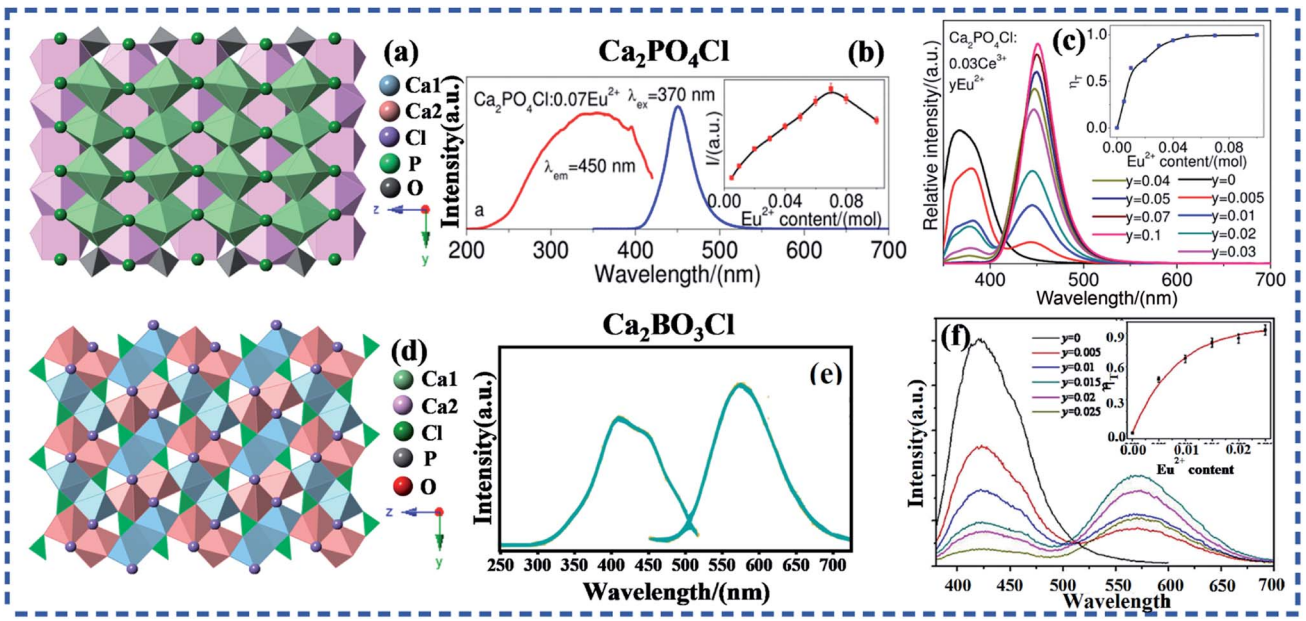

Fig. 6 (a) The crystal structure of Ca_2PO_4Cl. (b) The PL spectra of $Ca_2PO_4Cl:Eu^{2+}$ phosphors. (c) The PL spectra of a series of $Ca_2PO_4Cl:0.03Ce^{3+},yEu^{2+}$ phosphors with different Eu^{2+} concentrations excited at 370 nm. The inset shows the ET efficiency as a function of Eu^{2+} concentration in Ca_2PO_4Cl phosphors. (d) The crystal structure of Ca_2BO_3Cl. (e) The PL spectra of $Ca_2BO_3Cl:Eu^{2+}$ phosphors. (f) The PL spectra of a series of $Ca_2BO_3Cl:0.006Ce^{3+},yEu^{2+}$ phosphors with different Eu^{2+} concentrations excited at 320 nm. (Reproduced with permission from ref. 92 and 55, copyright 2014, 2019, *RSC Adv.*, *J. Mater. Sci.: Mater. Electron.*)

probability of ET between the same activator ions is reduced and the concentration quenching effect between activator ions is restricted to some degree.

The layered structure sometimes can be formed by selective occupation of activator ions in several hosts, which thus improves the luminescent properties of phosphors to a certain extent. It will be shown using the crystal structures of Ca_2PO_4Cl[92] and Ca_2BO_3Cl[55] as given in Fig. 6a and d. The Ca_2PO_4Cl crystallizes in the orthorhombic system with space group of *Pbcm*, and the crystal structure of Ca_2BO_3Cl belongs to the monoclinic system with space group of $P2_1/c$. There are two kinds of cationic sites (Ca1 and Ca2 sites) in Ca_2PO_4Cl and Ca_2BO_3Cl, as shown in Fig. 6a and d. The Ca1 and Ca2 sites of Ca_2PO_4Cl are arranged in layers, while in Ca_2BO_3Cl, the Ca1 and Ca2 sites are staggered. If the doped Eu^{2+} enter only one of the lattice sites, the far distance between the lattice sites will lower the probability of ET between activator ions, so the concentration quenching of Eu^{2+} does not occur easily when the doped concentration is low.

It can be seen from Fig. 6b that the emission spectrum of $Ca_2PO_4Cl:Eu^{2+}$ ranges from 400 to 530 nm under excitation at 370 nm, and the spectral profile of this emission are symmetrical with a relatively narrow full width at half maximum.[92] Thus, it is very likely that Eu^{2+} occupies only one of the cationic lattices after entering the host, and the luminescence intensity of Eu^{2+} does not quench when the doping concentration is $y = 0.1$, as can be seen from Fig. 6c.[92] This further confirms that Ce^{3+}–Eu^{2+} system has relatively high ET efficiency due to the relatively high QC of Eu^{2+} caused by the large distance between cationic lattices. However, the emission spectrum of $Ca_2BO_3Cl:Eu^{2+}$ contains asymmetrically broad emission band from 450 to 700 nm, which is ascribed to the two different sites of Eu^{2+}.[55] It can be seen from the structure diagram (Fig. 6d) that if the doped RE ions occupy both lattice sites, the distance between activator ions will be closer when the concentration of activator ions doped becomes larger. The energy will gradually dissipate due to the ET between different lattice sites and the same lattice sites, so the activator ion quenches when the doping concentration is low. In Ca_2BO_3Cl, the luminous intensity of Ce^{3+} decreased with the increase of Eu^{2+}, and the luminous intensity of Eu^{2+} increased first and then decreased with its maximum at $x = 0.015$.[55] Therefore, no matter in terms of the QC of Eu^{2+} or the actual ET efficiency from Ce^{3+} to Eu^{2+}, Ca_2PO_4Cl is superior to Ca_2BO_3Cl. This further shows the luminescence properties of phosphors can be improved by selective occupancy of activator ions.

3.2 Improving the luminescence properties of Ce^{3+}–Eu^{2+} co-doped phosphors by designing layered crystal structure

In addition to the above mentioned way of elective occupation of activator ions, choosing the host with layered crystal structure is also a method to improve the luminescence performance of phosphors. In recent years, many Ce^{3+}–Eu^{2+} co-doped hosts with layered structure have been reported, among which $BaMg_2(PO_4)_2$ (ref. 87) and $Ba_2Mg(BO_3)_2$ (ref. 86) are two representatives. Although the two hosts are both layered structure,

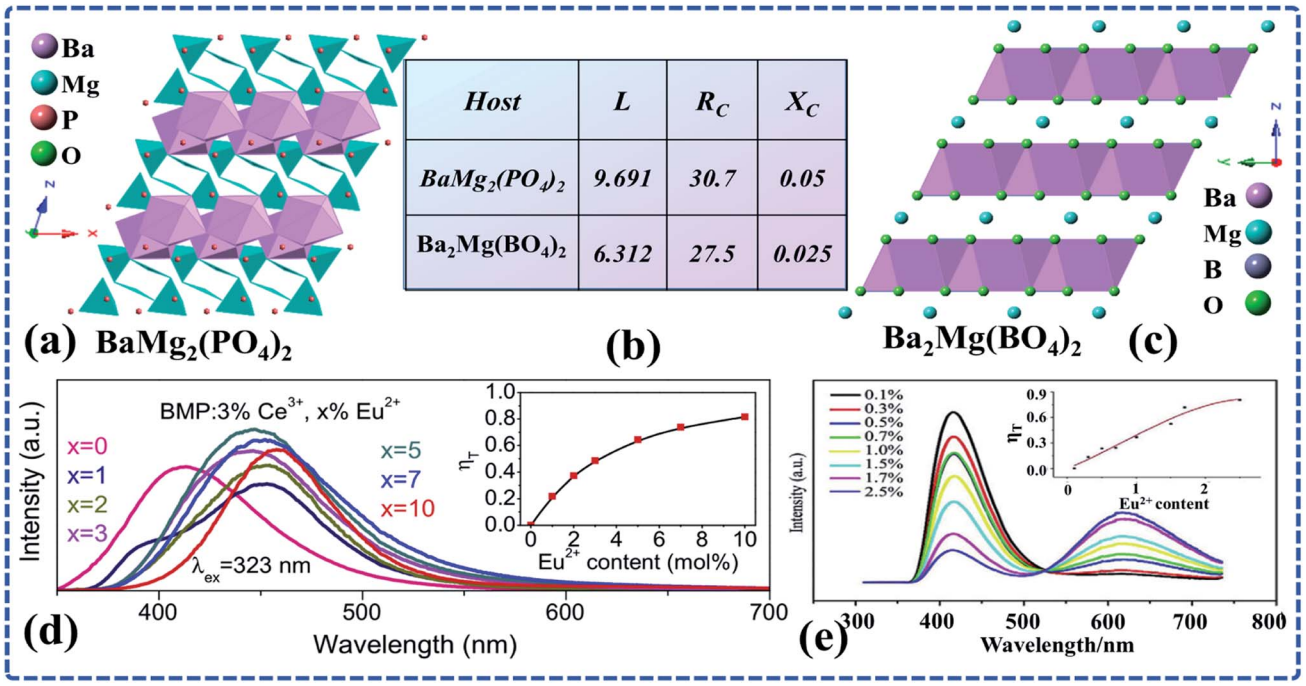

Fig. 7 (a) The crystal structure of $BaMg_2(PO_4)_2$. (b) The spacing between layers (L), critical distance (R_c) and quenching concentration (X_c) of $BaMg_2(PO_4)_2$ and $Ba_2Mg(BO_3)_2$. (c) The crystal structure of $Ba_2Mg(BO_3)_2$. (d) The photoluminescence emission (PL) spectra of a series of $BaMg_2(PO_4)_2$:3%Ce^{3+},*x*%Eu^{2+} phosphors with different Eu^{2+} concentrations excited at 323 nm. The inset shows the ET efficiency as a function of Eu^{2+} concentration in $BaMg_2(PO_4)_2$ phosphors. (e) PL spectra of a series of $Ba_2Mg(BO_3)_2$:2%Ce^{3+},*x*%Eu^{2+},2%Na^+ phosphors with different Eu^{2+} concentrations excited at 296 nm. (Reproduced with permission from ref. 87 and 86, copyright 2014, 2012, *J. Alloys Compd.*, *J. Rare Earths*.)

the crystal structures, the composition of cationic layers, and the distances between layers are all different. As can be seen from Fig. 7c and d, the luminous intensity of Ce^{3+} decreased with increasing Eu^{2+} doping concentration, while the luminous intensity of Eu^{2+} increased first and then decreased. Moreover, the actual ET efficiency from Ce^{3+} to Eu^{2+} in $BaMg_2(PO_4)_2$ is significantly higher than that in $Ba_2Mg(BO_3)_2$.[86,87] Therefore, it is reasonable to speculate that different distances between cationic layers cause different inhibition effects on the quenching of activator ions and thus different actual ET efficiency from Ce^{3+} to Eu^{2+}.

In fact, in addition to the above reasons, the critical distance between different hosts also affects QC effect. As shown in Fig. 7b, the distance between the cationic layers (Ba ions and Ba ions) in $BaMg_2(PO_4)_2$ is 9.691 Å, and the critical distance of ET from Ce^{3+} to Eu^{2+} system is 30.7 Å. When the doping concentration of Eu^{2+} is $x = 0.05$, the luminescence intensity of Eu^{2+} reaches its maximum.[87] In contrast, the distance between the cationic layers (Ba ions and Ba ions) in $Ba_2Mg(BO_3)_2$ is 6.312 Å, and the critical distance between Ce^{3+} and Eu^{2+} is 27.5 Å. When the doping concentration of Eu^{2+} is $x = 0.025$, the luminescence intensity of Eu^{2+} reaches its maximum.[86] It is obvious that $BaMg_2(PO_4)_2$ is better than $Ba_2Mg(BO_3)$ in terms of the distance between cationic layers, the critical distance between Ce^{3+} and Eu^{2+} and the QC of Eu^{2+}. In addition, the actual ET efficiency from Ce^{3+} to Eu^{2+} in $BaMg_2(PO_4)_2$ is significantly higher than that in $Ba_2Mg(BO_3)_2$. It further indicates that for the hosts with similar composition and crystal structure, a greater distance between layers can lower the ET probability caused by the close distance between the layers of the same activated ions, thus inhibiting the concentration quenching of activator ions and leading to higher doping concentration of activator ions. In addition, large critical distance between Ce^{3+} and Eu^{2+} ensures that the doping concentration of activator ions can be effectively increased in the range where the ET from Ce^{3+} to Eu^{2+} can happen, thus making the actual ET efficiency from Ce^{3+} to Eu^{2+} of $BaMg_2(PO_4)_2$ relatively high.

Although it has been mentioned above that the actual ET efficiency from Ce^{3+} to Eu^{2+} is relatively high in the hosts with layered crystal structure, it does not mean the hosts with layered structure always ensure a high actual ET efficiency of Ce^{3+}-to-Eu^{2+}. For example, the crystal structures of $Ca_2Mg_{0.25}Al_{1.5}Si_{1.25}O_7$ (ref. 46) and $Ca_2Mg_{0.5}Al_{1.5}Si_{1.5}O_7$ (ref. 4) as shown in Fig. 8a and b are all layered structures. It can be seen from the emission spectra presented in Fig. 8c and d that the luminous intensity of Ce^{3+} decreased greatly with the increase of Eu^{2+} doping concentration, whereas the Eu^{2+} emission only showed a slight increase, and the total emission intensity decreased. Obviously, the ET efficiency calculated according to the formula $\eta_{ET} = 1 - \frac{I_s}{I_{s0}}$ does not match the spectra.

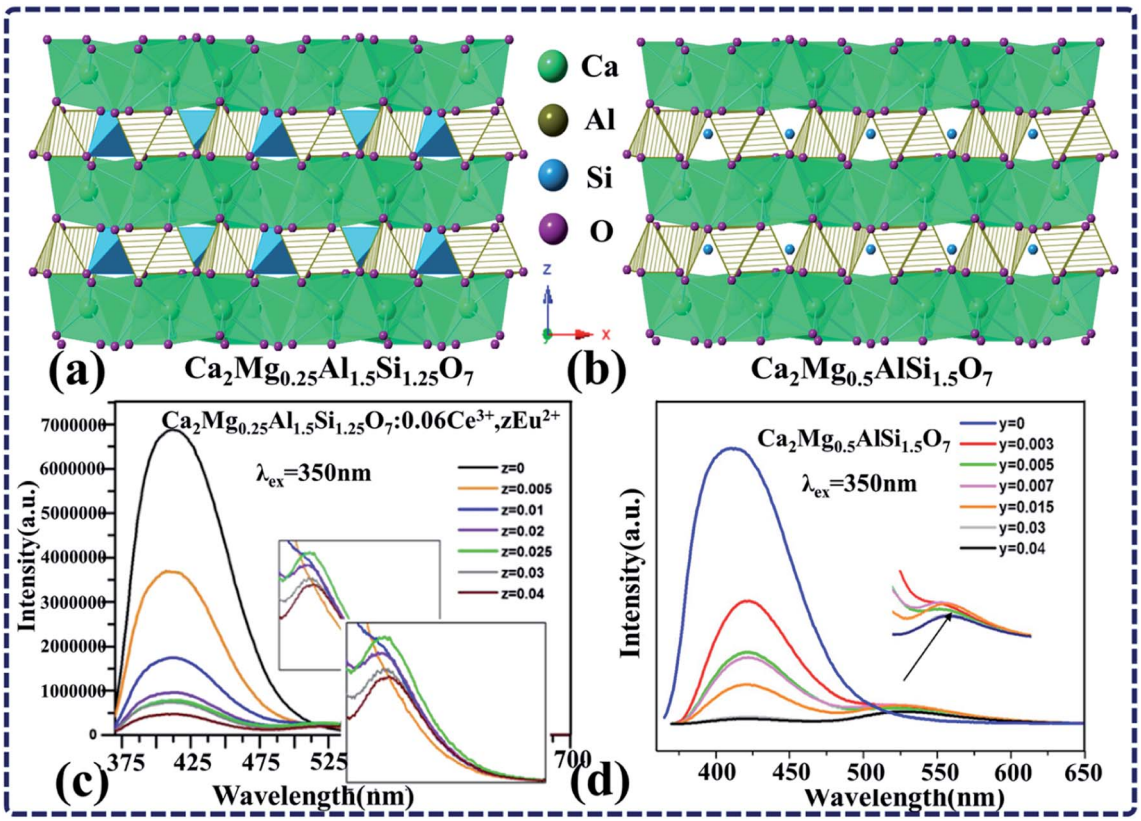

Fig. 8 (a) and (b) The crystal structure of $Ca_2Mg_{0.25}Al_{1.5}Si_{1.25}O_7$ and $Ca_2Mg_{0.5}Al_{1.5}Si_{1.5}O_7$. (c) The PL spectra of a series of $Ca_2Mg_{0.25}Al_{1.5}Si_{1.25}O_7$:0.06$Ce^{3+}$,y$Eu^{2+}$ with different Eu^{2+} concentrations excited at 350 nm. (d) PL spectra of a series of $Ca_2Mg_{0.5}Al_{1.5}Si_{1.5}O_7$:0.06$Ce^{3+}$,z$Eu^{2+}$ phosphors with different Eu^{2+} concentrations excited at 350 nm. (Reproduced with permission from ref. 46 and 4, copyright 2014, 2016, *Powder Technol. Lumin.*)

In order to clarify this problem, we analyzed the crystal structure and the information obtained from the reported literatures, concluding that the crystal structure of these two hosts is layered structure. Moreover, the distances between each two layers of $Ca_2Mg_{0.25}Al_{1.5}Si_{1.25}O_7$ (ref. 46) and $Ca_2Mg_{0.5}Al_{1.5}Si_{1.5}O_7$ (ref. 4) are separately 5.05 Å and 5.036 Å, the smallest distances of the layered structure hosts with connective bonds listed in this paper. Based on the previous discussion, this may be due to the fact that the distance between cationic layers is smaller and the distance between the same cation lattices is closer, thus increasing the probability of ET between activator ions. Therefore, the emission of Eu^{2+} is quenched at low doping concentration. As shown in Fig. 8c and d, the luminescence intensity of Eu^{2+} decreased with increasing doping concentration, which further verifies that even if the crystal structure of a host with high calculated ET efficiency from Ce^{3+} to Eu^{2+} is layered, its actual ET efficiency might be relatively low due to the small distance between layers. Therefore, not every host with layered crystal structure has good luminescence performance. When the spacing between layers is small, the distance between the same cations will be closer, thus increasing the probability of concentration quenching of activator ions. Therefore, the hosts with layered crystal structure and large spacing between layers are highly recommended when designing new phosphors in the future.

4. Summary and outlook

To sum up, the effect of crystal structure on the luminescence properties of phosphors is reviewed in this paper. It is found that the actual ET efficiency from Ce^{3+} to Eu^{2+} in the hosts with layered structure is higher than that with non-layered structure. It is because in these hosts with layered structure, the same cation lattice is far apart due to the special crystal structure, thus reducing the probability of ET caused by the close distance between activator ions and making the quenching concentration of activator ions relatively high. Therefore, the actual ET efficiency from Ce^{3+} to Eu^{2+} in these hosts is relatively high. Although the luminescence performance of the hosts with layered crystal structure is excellent, the ET efficiency from Ce^{3+} to Eu^{2+} in some hosts such as $Ca_2Mg_{0.25}Al_{1.5}Si_{1.25}O_7$ (ref. 46) and $Ca_2Mg_{0.5}Al_{1.5}Si_{1.5}O_7$ (ref. 4) is, however, not so ideal. It is because the spacing between layers is small, and the distance between the cation sites is close, which increases the probability of ET of activator ions and leads to concentration quenching when the doping concentration is small. In addition, it is also found that for some non-layered matrices, the luminescent properties can also be improved by the method of selective occupation of activator ions. By using this method, the crystal structure of hosts can be changed from cluster structure to layered or interstitial structure, which indirectly increases the distance between the same cation sites, restrains the activator ion concentration quenching, and make the emission efficiency of Eu^{2+} is higher, the luminous performance of phosphor material is better.

Over the past decades, great progress has been made in the field of WLED, especially the single-phase WLED excited by the near-ultraviolet radiation. Since the positions of the excited $4f^65d^1$ state relative to the ground state are strongly influenced by host lattice, the position of emission band depends strongly on the environmental conditions of Eu^{2+} and Ce^{3+} such as coordination number, bond length, crystal field splitting, the nephelauxetic effect, the Stokes shift, the distortion of host lattice and so forth. It thus varies between the near ultraviolet and near infrared spectral range. These works have been reviewed a lot, but there is no general rule applicable to all phosphor systems at present. Exploring the structure-related luminescence mechanism is still the focus of future research.

Although a particular emphasis is placed on Ce^{3+}–Eu^{2+} co-doped phosphors, we believe these theoretical approaches should be readily expandable to other lanthanide-doped systems with the characteristics of 4f–5d optical transitions, such as Ce^{3+}–Mn^{2+} and Eu^{2+}–Mn^{2+} co-doped systems. In addition, in some Ce^{3+}–Eu^{2+} co-doped phosphor, the crystal structure of host not only affects the QC of activator ions and the ET efficiency from Ce^{3+} to Eu^{2+}, but also affects the luminous color, thermal stability and quantum efficiency of phosphors. Therefore, these issues are also worthy of exploration, in order to meet different market demand for different performance LED.

It is worth noting that although the design of layered crystal structure and the selective occupation of activator ions can improve the luminescent properties of Ce^{3+}–Eu^{2+} co-doped phosphors, these rules do not apply to all Ce^{3+}–Eu^{2+} co-doped materials. The luminescence properties of phosphors are related not only to the crystal structure of host, but also to the overlapping degree of excitation spectrum of activator and emission spectra of sensitizer, synthesizing environment of materials, doping concentration of sensitizer and the critical distance between Ce^{3+} and Eu^{2+}. In conclusion, despite the many contributions to the development of Ce^{3+}–Eu^{2+} co-doped phosphors in recent years, there are still some open questions that need to make further study in the future.

Conflicts of interest

The authors declare no competing financial interest.

Acknowledgements

The work is supported by the National Natural Science Foundation of China (Nos 51672066, 51902080), the Funds for Distinguished Young Scientists of Hebei Province, China (No. A2018201101), and the Natural Science Foundation of Hebei Province, China (No. E2019201223), the personnel training project of Hebei Province, China (No. A201902005).

References

1 (*a*) J. H. Oh, S. J. Yang and Y. R. Do, *Light: Sci. Appl.*, 2014, **3**, e141; (*b*) H. Zhu, C. C. Lin, W. Luo, S. Shu, Z. Liu, Y. Liu, J. Kong, E. Ma, Y. Cao, R.-S. Liu and X. Chen, *Nat. Commun.*, 2014, **5**, 4312; (*c*) T. Pulli, T. Donsberg, T. Poikonen, F. Manoocheri, P. Karha and E. Ikonen, *Light: Sci. Appl.*, 2015, **4**, e332.

2 P. Li, Z. Wang, Z. Yang and Q. Guo, A novel, warm, white light-emitting phosphor Ca_2PO_4Cl: Eu^{2+}, Mn^{2+} for white LEDs, *J. Mater. Chem. C*, 2014, **2**, 7823–7829.

3 S. Liang, P. Dang, G. Li, M. S. Molokeev, Y. Wei, Y. Wei, H. Lian, M. Shang, A. A. Al Kheraiff and J. Lin, Controllable two-dimensional luminescence tuning in Eu^{2+}, Mn^{2+} doped $(Ca,Sr)_9Sc(PO_4)_7$ based on crystal field regulation and energy transfer, *J. Mater. Chem. C*, 2018, **6**, 6714–6725.

4 B. Yuan, Y. Song, Y. Sheng, K. Zheng, Q. Huo, X. Xu and H. Zou, Luminescence and energy transfer properties of color-tunable $Ca_2Mg_{0.25}Al_{1.5}Si_{1.25}O_7$: $Ce^{3+}/Eu^{2+}/Tb^{3+}$ phosphors for ultraviolet light-emitting diodes, *Luminescence*, 2016, **31**(2), 453–461.

5 C. Guo, X. Ding, L. Luan and Y. Xu, Two-color emitting of Eu^{2+} and Mn^{2+} co-doped $Sr_2Mg_3P_4O_{15}$ for UV LEDs, *Sens. Actuators, B*, 2010, **143**(2), 712–715.

6 C. Wang, P. Li, Z. Wang, Y. Sun, J. Cheng, Z. Li, M. Tian and Z. Yang, Crystal structure, luminescence properties, energy transfer and thermal properties of a novel color-tunable, white light-emitting phosphor $Ca_{9-x-y}Ce(PO_4)_7$: xEu^{2+}, yMn^{2+}, *Phys. Chem. Chem. Phys.*, 2016, **18**, 28661–28673.

7 C. Guo, X. Ding, H. Seo, Z. Ren and J. Bai, Double emitting phosphor $NaSr_4(BO_3)_3$: Ce^{3+}, Tb^{3+} for near-UV light-emitting diodes, *Opt. Laser Technol.*, 2011, **43**(7), 1351–1354.

8 N. Zhang, C. Guo, H. Jing and J. H. Jeong, Color tunable emission in Ce^{3+} and Tb^{3+} co-doped $Ba_2Ln(BO_3)_2Cl$ (Ln = Gd and Y) phosphors for white light-emitting diodes, *Spectrochim. Acta, Part A*, 2013, **116**, 556–561.

9 W. Tang and C. Ding, Luminescence Tuning of $Sr_8MgCe(PO_4)_7$: Eu^{2+}, Mn^{2+} Phosphors: Structure Refinement, Site Occupancy, and Energy Transfer, *Zeitschrift für anorganische und allgemeine Chemie*, 2018, **644**(16), 893–900.

10 X. Meng, K. Qiu, Z. Tian, X. Shi, J. You, Z. Wang, P. Li and Z. Yang, Tunable-emission single-phase phosphors $Ba_3Ca_2(PO_4)_3F$:M (M = Ce^{3+}, Eu^{2+}, Mn^{2+}): crystal structure, luminescence and energy transfer, *J. Alloys Compd.*, 2017, **719**, 322–330.

11 J. Yu, C. Guo, Z. Ren and J. Bai, Photoluminescence of double-color-emitting phosphor $Ca_5(PO_4)_3Cl$: Eu^{2+}, Mn^{2+} for near-UV LED, *Opt. Laser Technol.*, 2011, **43**(4), 762–766.

12 C. Wang, Z. Wang, P. Li, J. Cheng, Z. Li, M. Tian, Y. Sun and Z. Yang, Relationships between luminescence properties and polyhedron distortion in $Ca_{9-x-y-z}Mg_xSr_yBa_zCe(PO_4)_7$: Eu^{2+}, Mn^{2+}, *J. Mater. Chem. C*, 2017, **5**, 10839–10846.

13 L. Zhang, Z. Wang, C. Liu, G. Dong, D. Dai, Z. Xing, X. Li, Z. Yang and P. Li, Tunable emitting phosphor $Ca_6Ce_2Na_2(PO_4)_6F_2$: Mn^{2+}/Tb^{3+} for white LEDs: luminescence, energy transfer and high thermal property, *J. Lumin.*, 2020, **217**, 116817.

14 Q. Bao, Z. Wang, J. Sun, Z. Wang, X. Meng, K. Qiu, Y. Chen, Z. Yang and P. Li, Crystal structure, luminescence properties, energy transfer, tunable occupation and thermal properties of a novel color-tunable phosphor $NaBa_{1-z}Sr_zB_9O_{15}$: xCe^{3+}, yMn^{2+}, *Dalton Trans.*, 2018, **47**, 13913–13925.

15 J. Qiao, G. Zhou, Y. Zhou, Q. Zhang and Z. Xia, Divalent europium-doped near-infrared-emitting phosphor for light-emitting diodes, *Nat. Commun.*, 2019, **10**(1), 5267.

16 M. Zhang, Y. Liang, R. Tang, D. Yu, M. Tong, Q. Wang, Y. Zhu, X. Wu and G. Li, Highly Efficient $Sr_3Y_2(Si_3O_9)_2$: Ce^{3+}, $Tb^{3+}/Mn^{2+}/Eu^{2+}$ Phosphors for White LEDs: Structure Refinement, Color Tuning and Energy Transfer, *RSC Adv.*, 2014, **4**(76), 40626–40637.

17 R. Liu, Y. Liu, N. C. Bagkar and S. Hu, Enhanced luminescence of $SrSi_2O_2N_2$: Eu^{2+} phosphors by co-doping with Ce^{3+}, Mn^{2+}, and Dy^{3+} ions, *Appl. Phys. Lett.*, 2007, **91**(6), 061119–061119-3.

18 X. Jiang, Y. Zhang and J. Zhang, White-emission in single-phase $Ba_2Gd_2Si_4O_{13}$: Ce^{3+}, Eu^{2+}, Sm^{3+} phosphor for white-LEDs, *Spectrochim. Acta, Part A*, 2018, **192**, 194–201.

19 B. Cui, Z. Chen, Q. Zhang, H. Wang and Y. Li, A single-composition $CaSi_2O_2N_2$:RE (RE = Ce^{3+}/Tb^{3+}, Eu^{2+}, Mn^{2+}) phosphor nanofiber mat: energy transfer, luminescence and tunable color properties, *J. Solid State Chem.*, 2017, **253**, 263–269.

20 Z. Wei, Y. Wang, X. Zhu, J. Guan, W. Mao and J. Song, Solid state synthesis and tunable luminescence of Li_2SrSiO_4: Eu^{2+}/Ce^{3+} phosphors, *Chem. Phys. Lett.*, 2016, **648**, 8–12.

21 J. Zhao, X. Sun and Z. Wang, Ce^{3+}/Eu^{2+} doped $SrSc_2O_4$ phosphors: synthesis, luminescence and energy transfer from Ce^{3+} to Eu^{2+}, *Chem. Phys. Lett.*, 2018, **691**, 68–72.

22 W. Lv, J. Huo, Y. Feng, S. Zhao and H. You, Photoluminescence, energy transfer and tunable color of Ce^{3+}, Tb^{3+} and Eu^{2+} activated oxynitrides phosphor with high brightness, *Dalton Trans.*, 2016, **45**(23), 9676–9683.

23 J. Ha, Z. Wang, E. Novitskaya, G. A. Hirata, O. A. Graeve, S. P. Ong and J. McKittrick, An Integrated First Principles and Experimental Investigation of the Relationship between Structural Rigidity and Quantum Efficiency in Phosphors for Solid State Lighting, *J. Lumin.*, 2016, **179**, 297–305.

24 C. Guo, Y. Xu, F. Lv and X. Ding, Luminescent properties of Sr_2SiO_4: Eu^{2+} nanorods for near-UV white LED, *J. Alloys Compd.*, 2010, **497**(1–2), L21–L24.

25 G. Li, Y. Fan, H. Guo and Y. Wang, Synthesis, structure and photoluminescence properties of Ce^{3+}-doped $SrSc_2O_4$: a new scandate green-emitting phosphor with blue excitation, *New J. Chem.*, 2017, **41**, 5565–5571.

26 C. Guo, M. Li, Y. Xu, T. Li, Z. Ren and J. Bai, A potential green-emitting phosphor $Ca_8Mg(SiO_4)_4Cl_2$: Eu^{2+} for white light emitting diodes prepared by sol–gel method, *Appl. Surf. Sci.*, 2011, **257**(21), 8836–8839.

27 G. Li, Y. Zhao, Y. Wei, Y. Tian, Z. Quan and J. Lin, Novel yellowish-green light-emitting $Ca_{10}(PO_4)_6O$: Ce^{3+} phosphor: structural refinement, preferential site occupancy and color tuning, *Chem. Commun.*, 2016, **52**, 3376–3379.

28 J. Xiang, J. Zheng, Z. Zhou, H. Suo, X. Zhao, X. Zhou, N. Zhang, M. S. Molokeev and C. Guo, Enhancement of red emission and site analysis in Eu^{2+} doped new-type

structure $Ba_3CaK(PO_4)_3$ for plant growth white LEDs, *Chem. Eng. J.*, 2019, **356**, 236–244.

29 K. Uheda, N. Hirosaki, Y. Yamamoto, A. Naito, T. Nakajima and H. Yamamoto, Luminescence Properties of a Red Phosphor, $CaAlSiN_3$: Eu^{2+}, for White Light-Emitting Diodes, *Electrochem. Solid-State Lett.*, 2006, **9**, H22–H25.

30 P. Li, Z. Wang, Z. Yang and Q. Guo, $Ba_2B_2O_5$: Ce^{3+}: a novel blue emitting phosphor for white LEDs, *Mater. Res. Bull.*, 2014, **60**, 679–681.

31 Q. Wu, Z. Yang, Z. Zhao, M. Que, X. Wang and Y. Wang, Synthesis, crystal structure and luminescence properties of a $Y_4Si_2O_7N_2$: Ce^{3+} phosphor for near-UV white LEDs, *J. Mater. Chem. C*, 2014, **2**, 4967–4973.

32 R. Yu, C. Guo, T. Li and Y. Xu, Preparation and luminescence of blue-emitting phosphor Ca_2PO_4Cl: Eu^{2+} for n-UV white LEDs, *Curr. Appl. Phys.*, 2013, **13**(5), 880–884.

33 W. Geng, X. Zhou, J. Ding, G. Li and Y. Wang, $K_7Ca_9[Si_2O_7]_4F$: Ce^{3+}: a novel blue-emitting phosphor with good thermal stability for ultraviolet-excited light emitting diodes, *J. Mater. Chem. C*, 2017, **5**, 11605–11613.

34 X. Ding and Y. Wang, Structure and photoluminescence properties of a novel apatite green phosphor $Ba_5(PO_4)_2SiO_4$: Eu^{2+} excited by NUV light, *Phys. Chem. Chem. Phys.*, 2017, **19**, 2449–2458.

35 X. Wang, Z. Zhao, Q. Wu, C. Wang, Q. Wang, Y. Li and Y. Wang, Structure, photoluminescence and abnormal thermal quenching behavior of Eu^{2+}-doped $Na_3Sc_2(PO_4)_3$: a novel blue-emitting phosphor for n-UV LEDs, *J. Mater. Chem. C*, 2016, **4**, 8795–8801.

36 X. Wang, Z. Zhao, Q. Wu, Y. Li and Y. Wang, Synthesis, structure and photoluminescence properties of $Ca_2LuHf_2(AlO_4)_3$: Ce^{3+}, a novel garnet-based cyan light-emitting phosphor, *J. Mater. Chem. C*, 2016, **4**, 11396–11403.

37 Y. Liu, J. Zhang, C. Zhang, J. Xu, G. Liu, J. Jiang and H. Jiang, $Ba_9Lu_2Si_6O_{24}$: Ce^{3+}: An Efficient Green Phosphor with High Thermal and Radiation Stability for Solid-State Lighting, *Adv. Opt. Mater.*, 2015, **3**(8), 1096–1101.

38 Z. Wang, B. Yang, P. Li, Z. Yang and Q. Guo, Energy transfer between activators at different crystallographic sites in Sr_3SiO_5: Eu^{2+}, *Phys. B*, 2012, **407**(8), 1282–1286.

39 M. Zhang, J. Wang, Q. Zhang, W. Ding and Q. Su, Optical properties of Ba_2SiO_4: Eu^{2+} phosphor for green light-emitting diode (LED), *Mater. Res. Bull.*, 2007, **42**, 33–39.

40 W. Lv, Y. Jia, Q. Zhao, M. Jiao, B. Shao, W. Lü and H. You, Crystal Structure and Luminescence Properties of $Ca_8Mg_3Al_2Si_7O_{28}$: Eu^{2+} for WLEDs, *Adv. Opt. Mater.*, 2014, **2**, 183–188.

41 M. Zhao, Z. Xia, M. S. Molokeev, L. Ning and Q. Liu, Temperature and Eu^{2+} Doping Induced Phase Selection in $NaAlSiO_4$ Polymorphs and the Controlled Yellow/Blue Emission, *Chem. Mater.*, 2017, **29**, 6552–6559.

42 Z. Xia, R. Liu, K. Huang and V. Drozd, $Ca_2Al_3O_6F$: Eu^{2+}: a green-emitting oxyfluoride phosphor for white light-emitting diodes, *J. Mater. Chem.*, 2012, **22**, 15183–15189.

43 J. Qiao, L. Ning, M. S. Molokeev, Y. Chuang, Q. Liu and Z. Xia, Eu^{2+} Site Preferences in the Mixed Cation $K_2BaCa(PO_4)_2$ and Thermally Stable Luminescence, *J. Am. Chem. Soc.*, 2018, **140**(30), 9730–9736.

44 W. Sun, Y. Jia, R. Pang, H. Li, T. Ma, D. Li, J. Fu, S. Zhang, L. Jiang and C. Li, $Sr_9Mg_{1.5}(PO_4)_7$: Eu^{2+}: a novel broadband orange-yellow-emitting phosphor for blue light-excited warm white LEDs, *ACS Appl. Mater. Interfaces*, 2015, **7**(45), 25219–25226.

45 D. Zhao, S.-R. Zhang, Y.-P. Fan, B.-Z. Liu and R.-J. Zhang, Thermally Stable Phosphor $KBa_2(PO_3)_5$: Eu^{2+} with Broad-Band Cyan Emission Caused by Multisite Occupancy of Eu^{2+}, *Inorg. Chem.*, 2020, **59**, 8789–8799.

46 B. Yuan, Y. Song, Y. Sheng, K. Zheng, Q. Huo, X. Xu and H. Zou, Luminescence properties and energy transfer of $Ca_2Mg_{0.5}AlSi_{1.5}O_7$:$Ce^{3+}$, Eu^{2+} phosphors for UV-excited white LEDs, *Powder Technol.*, 2014, **253**, 803–808.

47 C. Ding and W. Tang, Crystal structure, energy transfer and tunable luminescence properties of $Ca_8ZnCe(PO_4)_7$: Eu^{2+}, Mn^{2+} phosphor, *Opt. Mater.*, 2018, **76**, 56–62.

48 C. Guo, Y. Xu, Z. Ren and J. Bai, Blue-White-Yellow Tunable Emission from Ce^{3+} and Eu^{2+} Co-Doped $BaSiO_3$ Phosphors, *J. Electrochem. Soc.*, 2011, **158**(12), J373–J376.

49 C. Li, H. Chen, Y. Hua, L. Yu, Q. Jiang, D. Deng, S. Zhao, H. Ma and S. Xu, Photoluminescence and energy transfer studies on Ce^{3+}/Eu^{2+} co-doped $Ba_3Si_6O_{12}N_2$ phosphor for white light-emitting-diodes, *Opt. Commun.*, 2013, **295**, 129–133.

50 C. Li, H. Zheng, H. Wei, S. Qiu, L. Xu, X. Wang and H. Jiao, A color tunable and white light emitting $Ca_2Si_5N_8$:Ce^{3+}, Eu^{2+} phosphor via efficient energy transfer for near-UV white LEDs, *Dalton Trans.*, 2018, **47**(19), 6860–6867.

51 C. Yang, Q. Liu, D. Huang, X. Li, X. Zhang, Z. Bai and X. Wang, Synthesis and luminescence properties of Eu^{2+}/Ce^{3+} co-doped $SrB_2Si_2O_8$ phosphor, *J. Mater. Sci.: Mater. Electron.*, 2019, **30**(6), 5544–5554.

52 C.-H. Huang, L. Luo and T.-M. Chen, An Investigation on the Luminescence and $Ce^{3+} \rightarrow Eu^{2+}$ Energy Transfer in $Ca_9Y(PO_4)_7$:Ce^{3+},Eu^{2+} Phosphor, *J. Electrochem. Soc.*, 2011, **158**(11), J341–J344.

53 C.-K. Chang and T.-M. Chen, $Sr_3B_2O_6$:Ce^{3+},Eu^{2+}: a potential single-phased white-emitting borate phosphor for ultraviolet light-emitting diodes, *Appl. Phys. Lett.*, 2007, **91**(8), 81902–81902-3.

54 F. Liu, Y. Tian, D. Deng, M. Wu, B. Chen, L. Zhou and S. Xu, An optical thermometer with high sensitivity and superior signal discriminability based on dual-emitting Ce^{3+}/Eu^{2+} co-doped $La_5Si_2BO_{13}$ thermochromic phosphor, *Journal of Rare Earths*, 2020, **10**, 3.

55 F. Xiao, Y. N. Xue and Q. Y. Zhang, Ca_2BO_3Cl:Ce^{3+},Eu^{2+}: a potential tunable yellow–white–blue-emitting phosphors for white light-emitting diodes, *Phys. B*, 2009, **404**(20), 3743–3747.

56 F. Zhang and W. Tang, Luminescence properties of Eu^{2+} and Ce^{3+} in $Na_5Ca_2Al(PO_4)_4$ produced by the combustion-assisted synthesis method, *J. Non-Cryst. Solids*, 2014, **389**, 46–49.

57 G. Li, M. Li, L. Li, H. Yu, H. Zou, L. Zou, S. Gan and X. Xu, Luminescent properties of $Sr_2Al_2SiO_7$:Ce^{3+},Eu^{2+} phosphors

for near UV-excited white light-emitting diodes, *Mater. Lett.*, 2011, **65**(23–24), 3418–3420.

58 G. Li and Y. Wang, Photoluminescence properties of novel $BaGd_2Si_3O_{10}$:$RE^{2+/3+}$ (RE = Eu or Ce) phosphors with trichromatic emission for white LEDs, *New J. Chem.*, 2017, **41**, 9178–9183.

59 H. Chen, C. Li, Y. Hua, L. Yu, Q. Jiang, D. Deng, S. Zhao, H. Ma and S. Xu, Influence of energy transfer from Ce^{3+} to Eu^{2+} on luminescence properties of $Ba_3Si_6O_9N_4$:Ce^{3+}, Eu^{2+} phosphors, *Ceram. Int.*, 2014, **40**(1), 1979–1983.

60 P. Thiyagarajan and M. S. Ramachandra Rao, Cool white light emission on $Ca_{3-(l+n)}MgSi_2O_8$:Ce^{3+}, Eu^{2+} phosphors and analysis of energy transfer mechanism, *Appl. Phys. A*, 2010, **99**, 947–953.

61 J. Hou, W. Jiang, Y. Fang and F. Huang, Red, green and blue emissions coexistence in white-light-emitting $Ca_{11}(SiO_4)_4(BO_3)_2$: Ce^{3+}, Eu^{2+}, Eu^{3+} phosphor, *J. Mater. Chem. C*, 2013, **1**, 5892–5898.

62 J. Sun, J. Zeng, Y. Sun and H. Du, Photoluminescence properties and energy transfer of Ce^{3+}, Eu^{2+} co-doped $Sr_3Gd(PO_4)_3$ phosphor, *J. Alloys Compd.*, 2012, **540**, 81–84.

63 J. Yan, C. Liu, W. Zhou, Y. Huang, Y. Tao and H. Liang, VUV-UV-vis photoluminescence of Ce^{3+} and Ce^{3+}-Eu^{2+} energy transfer in $Ba_2MgSi_2O_7$, *J. Lumin.*, 2017, **185**, 251–257.

64 L. Chen, R. Liu, W. Zhuang, Y. Liu, Y. Hu, X. Zhou and X. Ma, A study on photoluminescence and energy transfer of $SrAlSi_4N_7$:Eu^{2+}, Ce^{3+} phosphors for application in white-light LED, *J. Alloys Compd.*, 2015, **627**, 218–221.

65 L. Zhou, H. Liang, P. A. Tanner, S. Zhang, D. Hou, C. Liu, Y. Tao, Y. Huang and L. Li, Luminescence, cathodoluminescence and $Ce^{3+} \rightarrow Eu^{2+}$ energy transfer and emission enhancement in the $Sr_5(PO_4)_3Cl$:Ce^{3+},Eu^{2+} phosphor, *J. Mater. Chem. C*, 2013, **1**(43), 7155–7165.

66 M. Chen, Z. Xia, M. S. Molokeev and Q. Liu, Insights into $Ba_4Si_6O_{16}$ structure and photoluminescence tuning of $Ba_4Si_6O_{16}$:Ce^{3+},Eu^{2+} phosphors, *J. Mater. Chem. C*, 2015, **3**(48), 12477–12483.

67 W. Shen, Y. Zhu and Z. Wang, Luminescent properties of $Ca_3SiO_4Cl_2$ co-doped with Ce^{3+} and Eu^{2+} for near-ultraviolet light-emitting diodes, *Luminescence*, 2015, **30**, 1409–1412.

68 N. Lakshminarasimhan and U. V. Varadaraju, White-Light Generation in Sr_2SiO_4: Eu^{2+}, Ce^{3+} under Near-UV Excitation, *J. Electrochem. Soc.*, 2005, **152**(9), H152–H156.

69 P. Li, Z. Wang, Q. Guo and Z. Yang, Tunable Emission Phosphor $Ca_4Y_6O(SiO_4)_6$:Ce^{3+}, Eu^{2+}: Luminescence and Energy Transfer, *J. Am. Ceram. Soc.*, 2015, **98**(2), 495–500.

70 P. Li, Z. Wang, Z. Yang and Q. Guo, A potential single-phased white-emitting $LiBaBO_3$: Ce^{3+}, Eu^{2+} phosphor for white LEDs, *J. Rare Earths*, 2010, **28**(4), 523–525.

71 P. Thiyagarajan and M. S. Ramachandra Rao, Cool white light emission on $Ca_{3-(l+n)}MgSi_2O_8$: Ce_l^{3+}, Eu_n^{2+} phosphors and analysis of energy transfer mechanism, *Appl. Phys. A: Mater. Sci. Process.*, 2010, **99**(4), 947–953.

72 Q. Wang, D. Deng, Y. Hua, L. Huang, H. Wang, S. Zhao, G. Jia, C. Xia and S. Xu, Potential tunable white-emitting phosphor $LiSr_4(BO_3)_3$:Ce^{3+}, Eu^{2+} for ultraviolet light-emitting diodes, *J. Lumin.*, 2012, **132**(2), 434–438.

73 T. Li, P. Li, Z. Wang, S. Xu, Q. Bai and Z. Yang, Coexistence phenomenon of Ce^{3+}–Ce^{4+} and Eu^{2+}–Eu^{3+} in Ce/Eu co-doped $LiBaB_9O_{15}$ phosphor: luminescence and energy transfer, *Phys. Chem. Chem. Phys.*, 2017, **19**, 4131–4138.

74 V. Sivakumar and U. V. Varadaraju, Eu^{2+}, Ce^{3+} Luminescence and Ce^{3+}\Eu^{2+} Energy-Transfer Studies on Sr_2LiSiO_4F: A White Light-Emitting Phosphor, *J. Electrochem. Soc.*, 2009, **156**(7), J179–J184.

75 W. Lv, N. Guo, Y. Jia, Q. Zhao and H. You, A potential single-phased emission-tunable silicate phosphor $Ca_3Si_2O_7$: Ce^{3+}, Eu^{2+} excited by ultraviolet light for white light emitting diodes, *Opt. Mater.*, 2013, **35**(5), 1013–1018.

76 W. Wang, Y. Yang, Y. Liu, D. Pan, X. Luo, S. Yan, G. Xiang and Y. Jin, Photoluminescence properties and efficient energy transfer of Ce^{3+}/Eu^{2+} activated $K_2Ba_7Si_{16}O_{40}$ phosphors, *Mater. Res. Bull.*, 2018, **101**, 232–239.

77 W.-J. Yang and T.-M. Chen, Ce^{3+}/Eu^{2+} codoped Ba_2ZnS_3: a blue radiation-converting phosphor for white light-emitting diodes, *Appl. Phys. Lett.*, 2007, **90**(17), 171908–171908-3.

78 X. Meng, X. Jie, Y. Zhang, D. Wang, Y. Wang, P. Li and Z. Wang, Luminescence and energy transfer of Ce^{3+}-Eu^{2+} in $Ca_9Al(PO_4)_7$, *Optoelectronics Letters*, 2015, **11**(1), 45–48.

79 X. Song, R. Fu, S. Agathopoulos, H. He, X. Zhao and X. Yu, Synthesis of $BaSi_2O_2N_2$:Ce^{3+},Eu^{2+} Phosphors and Determination of their Luminescence Properties, *J. Am. Ceram. Soc.*, 2011, **94**(2), 501–507.

80 X. Tong, J. Han, Z. Cheng, P. Wu and X. Zhang, Efficient energy transfer induced tunable emission in Ce^{3+} and Eu^{2+} co-doped $Ba_{1.2}Ca_{0.8}SiO_4$ phosphor, *J. Lumin.*, 2019, **215**, 116670.

81 Y. Fang, L. Li, Y. Chen, H. Wang and R. Zeng, Photoluminescence properties of Ce^{3+} and Ce^{3+}–Eu^{2+} energy transfer in $Ba_{1.3}Ca_{0.7}SiO_4$ phosphors, *J. Lumin.*, 2013, **144**, 13–17.

82 Y. Jia, H. Qiao, Y. Zheng, N. Guo and H. You, Synthesis and photoluminescence properties of Ce^{3+} and Eu^{2+}-activated $Ca_7Mg(SiO_4)_4$ phosphors for solid state lighting, *Phys. Chem. Chem. Phys.*, 2012, **14**, 3537–3542.

83 Y. Jia, R. Pang, H. Li, W. Sun, J. Fu, L. Jiang, S. Zhang, Q. Su, C. Li and R.-S. Liu, Single-phased white-light-emitting $Ca_4(PO_4)_2O$:Ce^{3+}, Eu^{2+} phosphors based on energy transfer, *Dalton Trans.*, 2015, **44**, 11399–11407.

84 Y. Wang, J. Ding, Y. Wang, X. Zhou, Y. Cao, B. Ma, J. Li, X. Wang, T. Setoa and Z. Zhao, Structural design of new Ce^{3+}/Eu^{2+}-doped or co-doped phosphors with excellent thermal stabilities for WLEDs, *J. Mater. Chem. C*, 2019, **7**, 1792–1820.

85 Z. Hu, Z. Cheng, P. Dong, H. Zhang and Y. Zhang, Enhanced photoluminescence property of single-component $CaAlSiN_3$: Ce^{3+}, Eu^{2+} multicolor phosphor through Ce^{3+}-Eu^{2+} energy transfer, *J. Alloys Compd.*, 2017, **727**, 633–641.

86 Z. Pan, J. Xu, C. Zhu, W. Liu and L. Wang, $Ba_2Mg(BO_3)_2$:Ce^{3+},Eu^{2+},Na^+: a potential single-phased two

colour borate phosphor for white light-emitting diodes, *J. Rare Earths*, 2012, **30**(11), 1088–1091.

87 Z. Wang, X. Teng, P. Li, J. S. Lee, S. Unithrattil, W. B. Im, S. Ye, F. Xiao, Y. X. Pan and Y. Y. Ma, Luminescence and energy transfer of Ce^{3+}–Eu^{2+} in $BaMg_2(PO_4)_2$, *J. Alloys Compd.*, 2014, **589**, 549–552.

88 Z. Xia, S. Miao, M. Chen, M. S. Molokeev and Q. Liu, Structure, Crystallographic Sites, and Tunable Luminescence Properties of Eu^{2+} and Ce^{3+}/Li^{+}-Activated $Ca_{1.65}Sr_{0.35}SiO_4$ Phosphors, *Inorg. Chem.*, 2015, **54**, 7684–7691.

89 Z. Zhang and W. Tang, Efficient sensitization of Eu^{2+}/Mn^{2+} emissions by Ce^{3+} doping in $NaMgPO_4$ host under UV excitation, *Appl. Phys. A: Mater. Sci. Process.*, 2016, **122**(3), 229–237.

90 Z. Zhang and W. Tang, Tunable luminescence and energy transfer of $Ce^{3+}/Eu^{2+}/Mn^{2+}$-tridoped $Sr_8MgLa(PO_4)_7$ phosphor for white light LEDs, *J. Alloys Compd.*, 2016, **663**, 731–737.

91 H. He, R. Fu a, Y. Cao, X. Song, Z. Pan, X. Zhao, Q. Xiao and R. Li, Ce^{3+}, Eu^{2+} energy transfer mechanism in the Li_2SrSiO_4: Eu^{2+}, Ce^{3+} phosphor, *Opt. Mater.*, 2010, **32**, 632–636.

92 P. Li, Z. Wang, Z. Yang and Q. Guo, Incorporating Ce^{3+} into a high efficiency phosphor Ca_2PO_4Cl: Eu^{2+} and its luminescent properties, *RSC Adv.*, 2014, **4**, 27708–27713.

93 Y. Chen, Z. Wang, W. Ding, X. Li, Q. Bao, J. Liu, K. Qiu, X. Meng, Z. Yang and P. Li, A single-phase white light emitting phosphor $Ba_3Y(PO_4)_3$: $Ce^{3+}/Eu^{2+}/Mn^{2+}$: luminescence, energy transfer and thermal stability, *J. Lumin.*, 2019, **210**, 322–334.

94 G. Li, Y. Tian, Y. Zhao and J. Lin, Recent progress in luminescence tuning of Ce^{3+} and Eu^{2+} activated phosphors for pc-WLEDs, *Chem. Soc. Rev.*, 2015, **44**(23), 8688–8713.

95 H. Terraschke and C. Wickleder, UV, Blue, Green, Yellow, Red, and Small: Newest Developments on Eu^{2+}-Doped Nanophosphors, *Chem. Rev.*, 2015, **115**(20), 11352–11378.

96 Z. Xia and Q. Liu, Progress in discovery and structural design of color conversion phosphors for LEDs, *Prog. Mater. Sci.*, 2016, **84**, 59–117.

97 Z. Xia and K. R. Poeppelmeier, Chemistry-Inspired Adaptable Framework Structures, *Acc. Chem. Res.*, 2017, **50**, 1222–1230.

98 J. Qiao, J. Zhao, Q. Liu and Z. Xia, Recent advances in solid-state LED phosphors with thermally stable luminescence, *J. Rare Earths*, 2019, **37**, 565–572.

99 J. Qiao, J. Zhao and Z. Xia, (INVITED) A review on the Eu^{2+} doped β-$Ca_3(PO_4)_2$-type phosphors and the sites occupancy for photoluminescence tuning, *Opt. Mater.*, 2019, **1**, 100019.

100 X. Qin, X. Liu, W. Huang, M. Bettinelli and X. Liu, Lanthanide-Activated Phosphors Based on 4f-5d Optical Transitions: Theoretical and Experimental Aspects, *Chem. Rev.*, 2017, **117**(5), 4488–4527.

101 L. Wang, R.-J. Xie, T. Suehiro, T. Takeda and N. Hirosaki, Down-Conversion Nitride Materials for Solid State Lighting: Recent Advances and Perspectives, *Chem. Rev.*, 2018, **118**(4), 1951–2009.

102 C. Lin, A. Meijerink and R. S. Liu, Critical Red Components for Next-Generation White LEDs, *J. Phys. Chem. Lett.*, 2016, **7**, 495–503.

103 K. Li, M. Shang, H. Lian and J. Lin, Recent development in phosphors with different emitting colors via energy transfer for FEDs and UV/n-UV w-LEDs, *J. Mater. Chem. C*, 2016, **4**, 5507–5530.

104 M. Shang, C. Li and J. Lin, How to produce white light in a single-phase host, *Chem. Soc. Rev.*, 2014, **43**, 1372–1386.

105 C. Guo, Y. Xu, X. Ding, M. Li, J. Yu, Z. Ren and J. Bai, Blue-emitting phosphor $M_2B_5O_9Cl$: Eu^{2+} (M = Sr, Ca) for white LEDs, *J. Alloys Compd.*, 2011, **509**(4), L38–L41.

106 C. Tao, Z. Wang, Z. Li, N. Zhang, Z. Yang and P. Li, Blue emitting phosphor $Sr_{0.8}Ca_{0.2}Al_{2+y}Si_{2-y}O_8$: Ce^{3+}: substitution of Al-Si, structural modification, luminescence property and application, *J. Alloys Compd.*, 2019, **788**, 1000–1008.

107 J. Ding, H. You, Y. Wang, B. Ma, X. Zhou, X. Ding, Y. Cao, H. Chen, W. Geng and Y. Wang, Site occupation and energy transfer of Ce^{3+}-activated lithium nitridosilicate $Li_2SrSi_2N_4$ with broad-yellow-light-emitting property and excellent thermal stability, *J. Mater. Chem. C*, 2018, **6**, 3435–3444.

108 J. Liu, Z. Wang, X. Li, X. Meng, K. Qiu, D. Wang, J. Zhao, W. Lai, Z. Yang and P. Li, Achieving tunable emitting $YAl_3(BO_3)_4$: Eu phosphors by substituting cations (Sr^{2+}, Ca^{2+}, Ga^{3+}, In^{3+}) and controlling BO_3 group polarizability, *CrystEngComm*, 2020, **22**, 5323–5337.

109 J. Wang, S. Huang, M. Shang, P. Dang, H. Lian and J. Lin, The effect of local structure on the luminescence of Eu^{2+} in ternary phosphate solid solutions by cationic heterovalent substitution and their application in white LEDs, *J. Mater. Chem. C*, 2021, **9**, 3.

110 K. V. Terebilenko, S. G. Nedilko, V. P. Chornii, V. M. Prokopets, M. S. Slobodyanika and V. V. Boykob, Structural and optical properties of langbeinite-related red-emitting $K_2Sc_2(MoO_4)(PO_4)_2$: Eu phosphors, *RSC Adv.*, 2020, **10**, 25763–25772.

111 M. Amin, P. Strobel, A. Qamar, T. Giftthaler, W. Schnick and A. Moewes, Understanding of Luminescence Properties Using Direct Measurements on Eu^{2+}-Doped Wide Bandgap Phosphors, *Adv. Opt. Mater.*, 2020, **8**, 16.

112 M. Tian, Z. Wang, W. Li, C. Wang, J. Cheng, Z. Li, Z. Yang and P. Li, Regulation defect and Eu^{2+} luminescence via cation substitution in Ca_2BO_3Cl: Eu^{2+}, M^{2+} (M = Sr and Ba) for white LEDs, *J. Alloys Compd.*, 2019, **787**, 1004–1014.

113 M. Tian, Z. Wang, Z. Li, J. Cheng, C. Wang, X. Li, Z. Yang and P. Li, Excellent human eye sensitivity matching, high luminous efficacy, high quantum yield and thermal stability of narrow-band red-emitting $SrLiAl_3N_4$: Eu^{2+} phosphor, *J. Lumin.*, 2019, **207**, 545–552.

114 M. Zhao, Q. Zhang and Z. Xia, Structural Engineering of Eu^{2+} Doped Silicates Phosphors for LED Applications, *Acc. Mater. Res.*, 2020, **1**, 137–145.

115 P. Dang, G. Li, S. Liang, H. Lian and J. Lin, Multichannel photoluminescence tuning in Eu-doped apatite phosphors via coexisting cation substitution, energy transfer and valence mixing, *J. Mater. Chem. C*, 2019, **7**, 5975–5987.

116 P. Li, Z. Wang, Z. Li, J. Cheng, Y. Sun, C. Wang, X. Teng, Z. Yang and F. Teng, Controlling multi luminescent centers via anionic polyhedron substitution to achieve single Eu^{2+} activated high-color-rendering white light/tunable emissions in single-phased $Ca_2(BO_3)_{1-x}(PO_4)_xCl$ phosphors for ultraviolet converted LEDs, *Chem. Eng. J.*, 2017, **326**, 667–679.

117 Q. Bai, P. Li, Z. Wang, S. Xu, T. Li and Z. Yang, Tuning of luminescence properties by controlling an aid-sintering additive and composition in $Na(Ba/Sr/Ca)PO_4$: Eu^{2+} for white LEDs, *RSC Adv.*, 2017, **7**, 22301–22310.

118 Q. Bao, Z. Wang, Z. Wang, X. Meng, K. Qiu, Y. Chen, Y. Li, J. Sun, Z. Yang and P. Li, Role of H_3BO_3 and Sr^{2+}/K^+ in the luminescent property of $NaBaB_9O_{15}$: Eu^{2+}, *J. Lumin.*, 2020, **218**(30), 116840.

119 Q. Wei, X. Zhou, Z. Tang, X. Wang and Y. Wang, A novel blue-emitting Eu^{2+}-doped chlorine silicate phosphor with a narrow band for illumination and displays: structure and luminescence properties, *CrystEngComm*, 2019, **21**, 3660–3667.

120 Q. Wu, X. Wang, Z. Zhao, C. Wang, Y. Li, A. Maoa and Y. Wang, Synthesis and luminescence characteristics of nitride $Ca_{1.4}Al_{2.8}Si_{9.2}N_{16}$: Ce^{3+}, Li^+ for light-emitting devices and field emission displays, *J. Mater. Chem. C*, 2014, **2**, 7731–7738.

121 Q. Zhang, X. Wang, Z. Tang and Y. Wang, A $K_3ScSi_2O_7$: Eu^{2+} based phosphor with broad-band NIR emission and robust thermal stability for NIR pc-LEDs, *Chem. Commun.*, 2020, **56**, 4644–4647.

122 X. Li, P. Li, C. Liu, L. Zhang, D. Dai, Z. Xing, Z. Yang and Z. Wang, Tuning the luminescence of $Ca_9La(PO_4)_7$: Eu^{2+} via artificially inducing potential luminescence centers, *J. Mater. Chem. C*, 2019, **7**, 14601–14611.

123 Z. Li, T. Seto and Y. Wang, Enhanced crystallinity and thermal stability of Ba^{2+} and Al^{3+}–O^{2-} co-substituted $Sr_2Si_5N_8$: Eu^{2+}, *J. Mater. Chem. C*, 2020, **8**, 9874–9884.

124 Z. Li, Z. Wang, P. Li, J. Cheng, M. Tian, C. Wang and Z. Yang, Improvement of thermal stability and photoluminescence in $Sr_{0.8}Ca_{0.2}Al_2Si_2O_8$: Eu^{2+} by the substitution of Si–Na # Al–Sr and Ca # Sr for structural modifications, *Dalton Trans.*, 2017, **46**, 14310–14317.

125 Z. Xia, J. Zhuang, A. Meijerink and X. Jing, Host composition dependent tunable multicolor emission in the single-phase $Ba_2(Ln_{1-z}Tb_z)(BO_3)_2Cl$: Eu phosphors, *Dalton Trans.*, 2013, **42**, 6327–6336.

126 Z. Zhou, N. Zhang, J. Chen, X. Zhou, M. S. Molokeev and C. Guo, The Vis-NIR multicolor emitting phosphor $Ba_4Gd_3Na_3(PO_4)_6F_2$: Eu^{2+}, Pr^{3+} for LED towards plant growth, *J. Ind. Eng. Chem.*, 2018, **65**, 411–417.

127 H. Zhang, D. Yuan, X. Mi, X. Liu and J. Lin, Color tuning in $Ca_{3-x}M_x(PO_4)_2$: Eu^{2+} (M = Sr, Ba) phosphors via cation substitution, *Dalton Trans.*, 2020, **49**, 8949–8958.

128 Z. Xia, H. Liu, X. Li and C. Liu, Identification of the crystallographic sites of Eu^{2+} in $Ca_9NaMg(PO_4)_7$: structure and luminescence properties study, *Dalton Trans.*, 2013, **42**, 16588–16595.

129 Z. Wang, Z. Xia, M. S. Molokeev, V. V. Atuchin and Q. Liu, Blue-shift of Eu^{2+} emission in $(Ba,Sr)_3Lu(PO_4)_3$: Eu^{2+} eulytite solid-solution phosphors resulting from release of neighbouring-cation-induced stress, *Dalton Trans.*, 2014, **43**(44), 16800–16804.

130 Z. Qiu, H. Lian, M. Shang, S. Lian and J. Lin, The structural evolution and spectral blue shift of solid solution phosphors $Sr_{3-m}Ca_mB_2O_6$: Eu^{2+}, *CrystEngComm*, 2016, **18**, 4597–4603.

131 Y. Wei, X. Qi, H. Xiao, W. Luo, H. Yao, L. Lv, G. Li and J. Lin, Site-preferential occupancy induced photoluminescence tuning in $(Ca,Ba)_5(PO_4)_3Cl$: Eu^{2+} phosphors, *RSC Adv.*, 2016, **6**, 43771–43779.

132 Y. Wu, Q. Li, B. C. Chakoumakos, M. Zhuravleva, A. C. Lindsey, J. Johnson II, L. Stand, M. Koschan and C. L. Melcher, Quaternary Iodide $K(Ca,Sr)I_3$: Eu^{2+} Single-Crystal Scintillators for Radiation Detection: Crystal Structure, Electronic Structure, and Optical and Scintillation Properties, *Adv. Opt. Mater.*, 2016, **4**(10), 1518–1532.

133 S. Xin, M. Gao, C. Wang, X. Wang, G. Zhu, F. Zhou, Z. Lia and Y. Wang, Efficient and controllable photoluminescence in novel solid solution $Ca_{1-x}Sr_xHf_4(PO_4)_6$: Eu^{2+} phosphors with high thermal stability for white light emitting diodes, *CrystEngComm*, 2018, **20**, 4383–4394.

134 W. Ji, Z. Xia, K. Liu, S. Alikhan, L. Hao, X. Xu, L. Yin, M. S. Molokeev, S. Agathopoulos, W. Yang, X. Ma, K. Sun and I. Silva, Crystal structure and luminescence properties of a novel green-yellow emitting $Ca_{1.5}Mg_{0.5}Si_{1-x}Li_xO_{4-\delta}$: Ce^{3+} phosphor with high quantum efficiency and thermal stability, *Dalton Trans.*, 2018, 47.

135 S. Liu, Z. Wang, Q. Bao, X. Li, Y. Chen, Z. Wang, X. Meng, Y. Li, Z. Yang and P. Li, Determination of luminescence and occupy sites of Ce^{3+} in $Zn_3(BO_3)(PO_4)$ by introducing Ca^{2+} and Mg^{2+} ions, *Spectrochim. Acta, Part A*, 2019, **213**, 134–140.